

Maximum entropy principle explains quasistationary states in systems with long-range interactions: The example of the Hamiltonian mean-field model

Andrea Antoniazzi,¹ Duccio Fanelli,^{1,2} Julien Barré,³ Pierre-Henri Chavanis,⁴ Thierry Dauxois,⁵ and Stefano Ruffo¹

¹Dipartimento di Energetica and CSDC, Università di Firenze, and INFN, via S. Marta, 3, 50139 Firenze, Italy

²Department of Cell and Molecular Biology, Karolinska Institute, SE-171 77 Stockholm, Sweden

³Laboratoire J. A. Dieudonné, UMR CNRS 6621, Université de Nice Sophia-Antipolis Parc Valrose, 06108 Nice cédex 2, France

⁴Laboratoire de Physique Théorique, Université Paul Sabatier, 118, route de Narbonne 31062 Toulouse, France

⁵Laboratoire de Physique, UMR CNRS 5672, ENS Lyon, 46 Allée d'Italie, 69364 Lyon cédex 07, France

(Received 3 March 2006; published 12 January 2007)

A generic feature of systems with long-range interactions is the presence of *quasistationary* states with non-Gaussian single particle velocity distributions. For the case of the Hamiltonian mean-field model, we demonstrate that a maximum entropy principle applied to the associated Vlasov equation explains known features of such states for a wide range of initial conditions. We are able to reproduce velocity distribution functions with an analytic expression which is derived from the theory with no adjustable parameters. A normal diffusion of angles is detected, which is consistent with Gaussian tails of velocity distributions. A dynamical effect, two oscillating clusters surrounded by a halo, is also found and theoretically justified.

DOI: 10.1103/PhysRevE.75.011112

PACS number(s): 05.20.-y, 05.45.-a

Long-range interactions are common in nature [1]. Examples include: self-gravitating systems [2], plasmas [3], dipolar magnets [4], and wave-particle interactions [5]. Theoretical studies have shown that the thermodynamic properties of these systems differ from those of systems with short-range interactions. For instance, long-range interactions may produce a negative microcanonical specific heat [7] and, more generally, inequivalence of the canonical and microcanonical ensembles [8]. Also the dynamics of models with long-range interactions has been studied, revealing a variety of peculiar features such as the presence of breaking of ergodicity in microcanonical dynamics [9,10] and the existence of quasistationary states whose relaxation time to equilibrium diverges with system size [11,12]. A number of paradigmatic toy models have been proposed that provide the ideal ground for theoretical investigations. Among others, the Hamiltonian mean-field (HMF) model [11] is nowadays widely analyzed because it displays many features of the long-range interactions while being simple to study analytically and numerically. Besides that, this model finds its physical motivation as an approximate representation of one-dimensional self-gravitating systems and constitutes an excellent entry to the self-consistent Colson-Bonifacio description of the single-pass free electron laser [13]. Within the HMF scenario, non-Gaussian velocity distributions [14] and signatures of anomalous diffusion [15] have been reported in the literature. These discoveries have originated an intense debate about the general validity of Boltzmann-Gibbs statistical mechanics for systems with long-range interactions [6,16]. Non-Gaussian distributions have been *fitted* using Tsallis' q exponentials [17], i.e., algebraically decaying profiles predicted within the realm of nonextensive statistical mechanics. Based on these findings, the generalized thermodynamic formulation pioneered by Tsallis was proposed as a tool to describe the properties of quasistationary states that arise in the presence of long-range forces [14].

In this paper, we demonstrate that a maximum entropy principle inspired by Lynden-Bell's theory of "violent relax-

ation" for the Vlasov equation allows one to explain satisfactorily the numerical simulations performed for the HMF model. Analytically obtained PDF's are superimposed to the numerics *without* adjusting any free parameter. In other words, our results point to the fact that *there is no need* to invoke generalized forms of Boltzmann-Gibbs statistical mechanics to describe the nonequilibrium properties of the broad class of long-range interacting systems. The HMF model describes the motion of N coupled rotators and is characterized by the following Hamiltonian:

$$H = \frac{1}{2} \sum_{j=1}^N p_j^2 + \frac{1}{2N} \sum_{i,j=1}^N [1 - \cos(\theta_j - \theta_i)], \quad (1)$$

where θ_j represents the orientation of the j th rotor and p_j is its conjugate momentum. To monitor the evolution of the system, it is customary to introduce the magnetization, a global order parameter defined as $M = |\mathbf{M}| = |\sum \mathbf{m}_i|/N$, where $\mathbf{m}_i = (\cos \theta_i, \sin \theta_i)$ is the local magnetization vector. Starting from *out-of-equilibrium* initial conditions, the system gets trapped in quasistationary states (QSS), whose lifetime diverges when increasing the number of particles N . Importantly, when performing the thermodynamic limit ($N \rightarrow \infty$) *before* the infinite time limit, the system cannot relax toward the Boltzmann-Gibbs equilibrium and remains permanently confined in QSS. In this regime, the magnetization is lower than predicted by the Boltzmann-Gibbs equilibrium and the system apparently displays a number of intriguing anomalies, e.g., non-Gaussian velocity distributions [14] and non-standard diffusion in angle [15]. We shall here provide strong evidence that the above phenomena can be successfully interpreted in the framework of the statistical theory of the Vlasov equation, a general approach originally introduced in the astrophysical and two-dimensional (2D) Euler turbulence contexts [18,19].

First, let us recall that for mean-field Hamiltonians such as (1), it has been rigorously proven [20] that, in the $N \rightarrow \infty$

limit, the N -particle dynamics is described by the Vlasov equation

$$\frac{\partial f}{\partial t} + p \frac{\partial f}{\partial \theta} - \frac{dV}{d\theta} \frac{\partial f}{\partial p} = 0, \quad (2)$$

where $f(\theta, p, t)$ is the microscopic one-particle distribution function and

$$V(\theta)[f] = 1 - M_x[f] \cos(\theta) - M_y[f] \sin(\theta), \quad (3)$$

$$M_x[f] = \int_{-\pi}^{\pi} \int_{-\infty}^{\infty} f(\theta, p, t) \cos \theta d\theta dp, \quad (4)$$

$$M_y[f] = \int_{-\pi}^{\pi} \int_{-\infty}^{\infty} f(\theta, p, t) \sin \theta d\theta dp. \quad (5)$$

The specific energy $h[f] = \int \int (p^2/2) f(\theta, p, t) d\theta dp - (M_x^2 + M_y^2 - 1)/2$ and momentum $P[f] = \int \int p f(\theta, p, t) d\theta dp$ functionals are conserved and given by their initial value.

We now turn to illustrate the maximum entropy method. The basic idea is to coarse-grain the microscopic one-particle distribution function $f(\theta, p, t)$ into a given set of values. It is then possible to associate an entropy to the coarse-grained distribution \bar{f} , i.e., averaged over a box of finite size, and statistical equilibrium can be determined by maximizing this entropy while imposing the conservation of certain Vlasov dynamical invariants. A detailed description of this procedure can be found in Ref. [21] in the context of two-dimensional Euler hydrodynamics.

In the following, we shall assume that the initial single particle distribution takes only two distinct values, namely $f_0 = 1/(4\Delta_\theta\Delta_p)$, if the angles (velocities) lie within an interval centered around zero and of half-width Δ_θ (Δ_p), and is zero otherwise. This choice corresponds to the so-called “water-bag” distribution which is fully specified by energy $h[f] = e$, momentum $P[f] = \sigma$, and initial magnetization $\mathbf{M}_0 = (M_{x0}, M_{y0})$. Vlasov time evolution can modify the shape of the boundary of the water-bag, while conserving the area inside it. Hence, the distribution remains two-level $(0, f_0)$ as time progresses. Coarse-graining amounts to performing a local average of f inside a given box and this procedure results in \bar{f} . The mixing entropy per particle associated with \bar{f} then reads

$$s(\bar{f}) = - \int dp d\theta \left[\frac{\bar{f}}{f_0} \ln \frac{\bar{f}}{f_0} + \left(1 - \frac{\bar{f}}{f_0}\right) \ln \left(1 - \frac{\bar{f}}{f_0}\right) \right]. \quad (6)$$

The shape of this entropy comes from a simple combinatorial analysis [7]. The maximum entropy principle is then defined by the following constrained variational problem:

$$S(e, \sigma) = \max_{\bar{f}} \left(s(\bar{f}) | h(\bar{f}) = e; P(\bar{f}) = \sigma; \int d\theta dp \bar{f} = 1 \right). \quad (7)$$

The problem is solved by introducing three Lagrange multipliers β/f_0 , λ/f_0 , and μ/f_0 for energy, momentum, and normalization. This leads to the following analytical form of the distribution:

$$\bar{f}(\theta, p) = f_0 \frac{e^{-\beta(p^2/2 - M_y[\bar{f}] \sin \theta - M_x[\bar{f}] \cos \theta) - \lambda p - \mu}}{1 + e^{-\beta(p^2/2 - M_y[\bar{f}] \sin \theta - M_x[\bar{f}] \cos \theta) - \lambda p - \mu}}. \quad (8)$$

This distribution differs from the Boltzmann-Gibbs one because of the “fermionic” denominator which is originated by the choice (6) of the entropy. Inserting expression (8) into the energy, momentum, and normalization constraints and using the definition of the magnetization, it can be straightforwardly shown that the momentum multiplier vanishes, $\lambda = 0$. Moreover, defining $x = e^{-\mu}$ and $\mathbf{m} = (\cos \theta, \sin \theta)$, yields the following system of implicit equations in the unknowns β , x , M_x and M_y :

$$f_0 \frac{x}{\sqrt{\beta}} \int d\theta e^{\beta \mathbf{M} \cdot \mathbf{m}} F_0(x e^{\beta \mathbf{M} \cdot \mathbf{m}}) = 1, \quad (9)$$

$$f_0 \frac{x}{2\beta^{3/2}} \int d\theta e^{\beta \mathbf{M} \cdot \mathbf{m}} F_2(x e^{\beta \mathbf{M} \cdot \mathbf{m}}) = e + \frac{M^2 - 1}{2},$$

$$f_0 \frac{x}{\sqrt{\beta}} \int d\theta \cos \theta e^{\beta \mathbf{M} \cdot \mathbf{m}} F_0(x e^{\beta \mathbf{M} \cdot \mathbf{m}}) = M_x,$$

$$f_0 \frac{x}{\sqrt{\beta}} \int d\theta \sin \theta e^{\beta \mathbf{M} \cdot \mathbf{m}} F_0(x e^{\beta \mathbf{M} \cdot \mathbf{m}}) = M_y,$$

with $F_0(y) = \int \exp(-v^2/2) / [1 + y \exp(-v^2/2)] dv$, $F_2(y) = \int v^2 \exp(-v^2/2) / [1 + y \exp(-v^2/2)] dv$, where v is a dummy variable. This system of equations is then solved using a Newton-Raphson method and the integrals involved are also performed numerically. For $e = \lim_{N \rightarrow \infty} H/N = 0.69$, a value often considered in the literature [24], the maximum entropy state has zero magnetization, for *any initial magnetization* $M_0 = |\mathbf{M}_0| < M_{crit} = 0.897$. Hence, the QSS distribution does not depend on the angles and the velocity distribution can be simplified into

$$f_{QSS}(p) = f_0 \frac{e^{-\beta p^2/2 - \mu}}{1 + e^{-\beta p^2/2 - \mu}}, \quad (10)$$

with β and μ numerically determined from system (9). Velocity profiles predicted by (10) are displayed in Fig. 1(a) for different values of the initial magnetization. Gaussian tails are always present, contrary to the power-law (q exponential) fits reported in Ref. [14]. Note that the power-law decay was already excluded on the basis of numerical simulations in Ref. [22] for initial zero magnetization states. At $M_0 = M_{crit} = 0.897$, a bifurcation occurs [see Fig. 1(b)] and the magnetization of the quasistationary state M_{QSS} becomes nonzero, which means that the equilibrium Lynden-Bell distribution develops an inhomogeneity in angles. The details of this phase transition are further discussed in Ref. [23].

We validate our theoretical findings in the initial magnetization range $M_0 \in [0, M_{crit}]$, by performing numerical simulations with N ranging from 10^3 to 10^7 . Numerical velocity distributions are compared in Fig. 2 with the analytical solution (10). Although not a single free parameter is used, we

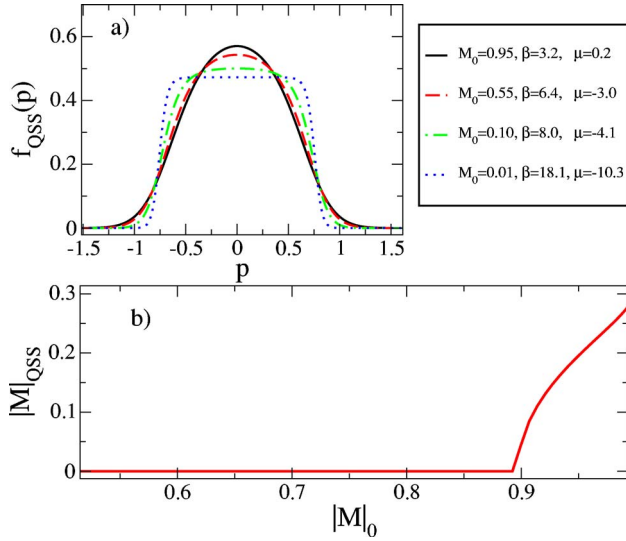


FIG. 1. (Color online) (a) Velocity profiles (10) predicted theoretically for different initial magnetizations (see legend, where we have reported also the values of the parameter β and μ). (b) final magnetization as a function of M_0 . A phase transition is observed at $M_0 = 0.897$ for $e = H/N = 0.69$.

find an excellent agreement in the tails of the distribution. The discrepancies observed in the center of the distributions are commented below.

To discuss the behavior of M in the QSS, one must distinguish different magnetization intervals. Consider first the interval $M_0 \in [M_a, M_{\text{crit}}]$, with $M_a \approx 0.5$. Both M_x and M_y are found to approach zero when the number of rotators is increased, in agreement with the theory outlined above. Our results correlate well with the scaling $|M| \propto N^{-1/6}$ reported in Ref. [24]. Numerical simulations also confirm the presence of a bifurcation at $M_0 = M_{\text{crit}}$, and indicate that the distribution in angles is indeed inhomogeneous above this value.

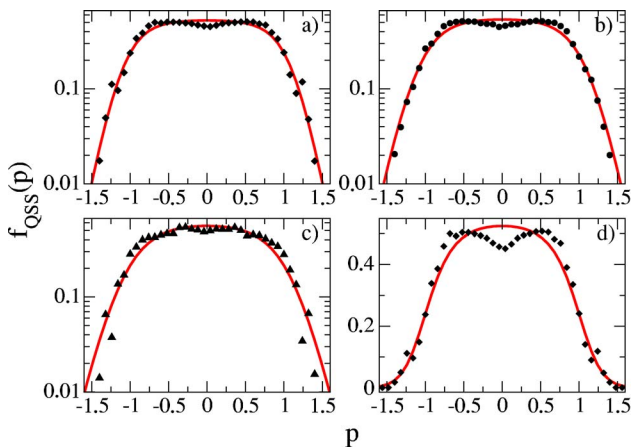


FIG. 2. (Color online) Velocity distribution functions. Symbols refer to numerical simulations, while dashed solid lines stand for the theoretical profile (10). Panels (a), (b), and (c) present the three cases $M_0 = 0.3$, $M_0 = 0.5$, and $M_0 = 0.7$ in lin-log scale, while panel (d) shows the case $M_0 = 0.3$ in lin-lin scale. The numerical curves are computed from one single realization with $N = 10^7$ at time $t = 100$. Here $e = H/N = 0.69$.

Interestingly, when the initial magnetization lies instead in the interval $[0, M_a]$, M_x and M_y display regular oscillations in time, which appear only when a large enough number of rotators ($N > 10^6$) is simulated. It is important to emphasize that the oscillations are centered around zero, i.e., the equilibrium value predicted by our theory. This feature shares striking similarities with the evolution of the laser intensity in the Bonifacio-Colson model [13].

We now discuss the presence of two symmetric bumps in the velocity distributions obtained numerically (see Fig. 2). This is a consequence of a collective phenomenon which leads to the formation of two clusters in the (θ, p) plane. Both clusters form early in time and then acquire constant opposite velocities which are maintained during the following time evolution. Hence, the clusters migrate away from their initial spatial locations and enlarge their relative separation. Consequently, the bumps displayed by the velocity distributions are not transient features, but represent instead an intrinsic peculiarity of QSS. When increasing the initial magnetization M_0 , the relative velocity decreases and the two clusters tend to merge. To the best of our knowledge, this is a collective phenomenon which has not been previously detected. A simple dynamical argument can be elaborated to shed light onto the process of formation of the clusters. Consider the one-particle Hamiltonian $\epsilon(\theta, p) = \frac{p^2}{2} - M_x \cos \theta - M_y \sin \theta$ associated to (1), where (θ, p) are the conjugate variables of the selected rotor. For short times, $\theta \sim \theta_0 + p_0 t$. One then finds $M_x \approx (\sin \Delta_\theta \sin \Delta_p t) / (\Delta_\theta \Delta_p t)$ and $M_y \approx 0$. Using this result, one ends up with

$$\epsilon(\theta, p) = \frac{p^2}{2} + \frac{\sin \Delta_\theta}{2 \Delta_\theta \Delta_p t} [\sin(\theta - \Delta_p t) + \sin(\theta + \Delta_p t)], \quad (11)$$

which corresponds to the Hamiltonian of one particle interacting with two waves of phase velocities $\pm \Delta_p$. Depending on the initial condition, the particles can be trapped in one of the two resonances, the latter being therefore directly responsible for the arising of two highly populated regions. Moreover, by including higher order corrections to the above calculation one can show that the two resonances tend to overlap when $M_0 \rightarrow 1$, in agreement with our numerical findings.

Having derived an analytical expression for the velocity distribution function (10), which is fully validated by the numerics, enables to take advantage of the predictions recently obtained in Ref. [25] using Klimontovich's approach. In [25] it was demonstrated that the momentum autocorrelation function can be deduced by knowing *only* the tails of the velocity distributions. The latter being shown above to be always Gaussian [see Eq. (10)], the momentum autocorrelation $\langle p(t)p(0) \rangle$, is expected to decay as $\ln t/t$. Here the brackets represent the average over N rotators. The mean square displacement of the angles $\sigma^2(t) = \langle |\theta_i(t) - \theta_i(0)|^2 \rangle$ is also a quantity of interest. The scaling $\sigma^2 \propto t^\gamma$ defines the diffusion behavior: $\gamma = 1$ corresponds to normal diffusion and $\gamma = 2$ to free particle ballistic dynamics. Intermediate cases correspond to the anomalous diffusion behavior. Here, for any water-bag initial conditions, the behavior of the momentum

autocorrelation function implies [25] that a weakly anomalous diffusion has to be expected, with a diffusion exponent $\gamma=1$ and logarithmic corrections. On the numerical simulations side, it is claimed in Ref. [24] that the QSSs of HMF display anomalous diffusion with an exponent γ in the range 1.4–1.5 for $0.4 \leq M_0 \leq 1$. These results are contradicted by more recent papers [26], where normal diffusion behavior is found. To provide further insight, we have monitored the time evolution of σ^2 by employing a larger number of particles ($N=10^5$) than in previous investigations. As clearly demonstrated by inspection of Fig. 3, a large value of the exponent γ is clearly excluded. On the contrary, the almost normal diffusion found is in complete agreement with the theoretical scenario discussed above.

In this paper, by drawing analogies with the statistical theory of violent relaxation in astrophysics and 2D Euler turbulence, we have analytically derived known properties of the quasistationary states of the HMF model. In particular: (i) velocity probability distributions in all quasistationary states investigated are accurately described by Lynden-Bell statistics (10); (ii) Gaussian tails of such maximum entropy states ensure an algebraic decay of momentum autocorrelation functions and, hence, a normal diffusion of the angles. Our theoretical approach is *fully predictive*, contrary to results obtained using nonextensive thermostats, which consist in *parametric fits* that are not justified from first principles. Despite this success of violent relaxation theory, we do not expect it to be so precise in all long-range systems: due to incomplete relaxation of the Vlasov equation [18,19], the QSS should deviate somewhat from Lynden-Bell's statistical prediction. Besides that, we have discovered that a double cluster spontaneously forms for all magnetizations. This collective effect was not known before. Our maximum

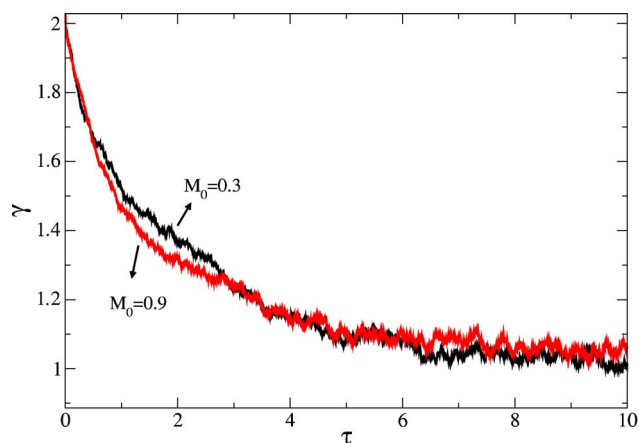


FIG. 3. (Color online) The exponent $\gamma=d \log(\sigma^2)/d \log(t)$ is plotted as a function of the rescaled time $\tau=t/N$. Starting from the initial ballistic value 2, it converges to the normal diffusion exponent 1. Simulations refer to $M_0=0.3$, and $M_0=0.9$. Here $N=10^5$ and $e=H/N=0.69$.

entropy principle is unable to capture this phenomenon, for which we have developed an analytical approach based on analogies with similar effects encountered in plasma-wave Hamiltonian dynamics. More refined maximum entropy schemes, accounting for the conservation of additional invariants besides the mass, are expected to give a full description of these phenomena and represent a challenge for future investigations.

We acknowledge financial support from the PRIN05-MIUR project *Dynamics and thermodynamics of systems with long-range interactions*.

-
- [1] T. Dauxois, S. Ruffo, E. Arimondo, and M. Wilkens, *Dynamics and Thermodynamics of Systems with Long Range Interactions*, Lecture Notes In Physics Vol. 602 (Springer, Berlin, 2002).
- [2] T. Padmanabhan, Phys. Rep. **188**, 285 (1990).
- [3] D. R. Nicholson, *Introduction to Plasma Physics* (Krieger Publishing Company, Florida, 1992).
- [4] G. I. Mias and S. M. Girvin, Phys. Rev. B **72**, 064411 (2005); L. Q. English, M. Sato, and A. J. Sievers, *ibid.* **67**, 024403 (2003).
- [5] J. Barré, T. Dauxois, G. DeNinno, D. Fanelli, and S. Ruffo, Phys. Rev. E **69**, 045501(R) (2004).
- [6] J. Barré *et al.*, Physica A **365**, 177 (2006).
- [7] D. Lynden-Bell and R. Wood, Mon. Not. R. Astron. Soc. **138**, 495 (1968).
- [8] J. Barré, D. Mukamel, and S. Ruffo, Phys. Rev. Lett. **87**, 030601 (2001).
- [9] F. Borgonovi *et al.*, J. Stat. Phys. **116**, 235 (2004).
- [10] D. Mukamel, S. Ruffo, and N. Schfieber, Phys. Rev. Lett. **95**, 240604 (2005).
- [11] M. Antoni and S. Ruffo, Phys. Rev. E **52**, 2361 (1995).
- [12] A. Taruya and M. A. Sakagami, Phys. Rev. Lett. **90**, 181101 (2003).
- [13] W. B. Colson, Phys. Lett. **59**, 187 (1976); R. Bonifacio *et al.*, Opt. Commun. **50**, 373 (1984).
- [14] V. Latora, A. Rapisarda, and C. Tsallis, Phys. Rev. E **64**, 056134 (2001).
- [15] V. Latora, A. Rapisarda, and S. Ruffo, Phys. Rev. Lett. **83**, 2104 (1999).
- [16] J. P. Boon and C. Tsallis, eds., Europhys. News **36** (2005).
- [17] C. Tsallis, J. Stat. Phys. **52**, 479 (1988).
- [18] D. Lynden-Bell, Mon. Not. R. Astron. Soc. **136**, 101 (1967).
- [19] P. H. Chavanis *et al.*, Astrophys. J. **471**, 385 (1996); P. H. Chavanis, Physica A **365**, 102 (2006).
- [20] W. Braun and K. Hepp, Commun. Math. Phys. **56**, 101 (1977).
- [21] J. Michel and R. Robert, Commun. Math. Phys. **159**, 195 (1994).
- [22] Y. Y. Yamaguchi *et al.*, Physica A **337**, 36 (2004).
- [23] P. H. Chavanis, Eur. Phys. J. B **53**, 487 (2006).
- [24] A. Pluchino, V. Latora, and A. Rapisarda, Phys. Rev. E **69**, 056113 (2004).
- [25] F. Bouchet and T. Dauxois, Phys. Rev. E **72**, 045103(R) (2005).
- [26] Y. Y. Yamaguchi, Phys. Rev. E **68**, 066210 (2003); L. G. Moyano and C. Anteneodo, Phys. Rev. E **74**, 021118 (2006).